

Energy evaluation of rammed earth walls using long term in-situ measurements

Soudani, L, Woloszyn, M, Fabbri, A, Morel, J-C & Grillet, A-C

Author post-print (accepted) deposited by Coventry University's Repository

Original citation & hyperlink:

Soudani, L, Woloszyn, M, Fabbri, A, Morel, J-C & Grillet, A-C 2016, 'Energy evaluation of rammed earth walls using long term in-situ measurements' *Solar Energy*, vol 141, no. January, pp. 70-80. DOI: 10.1016/j.solener.2016.11.002

<https://dx.doi.org/10.1016/j.solener.2016.11.002>

DOI 10.1016/j.solener.2016.11.002

ISSN 0038-092X

ESSN 1471-1257

Publisher: Elsevier

NOTICE: this is the author's version of a work that was accepted for publication in Solar Energy. Changes resulting from the publishing process, such as peer review, editing, corrections, structural formatting, and other quality control mechanisms may not be reflected in this document. Changes may have been made to this work since it was submitted for publication. A definitive version was subsequently published in Solar Energy, [141 Jan (2016)] DOI: 10.1016/j.solener.2016.11.002

© 2016, Elsevier. Licensed under the Creative Commons Attribution-NonCommercial-NoDerivatives 4.0 International <http://creativecommons.org/licenses/by-nc-nd/4.0/>

Copyright © and Moral Rights are retained by the author(s) and/ or other copyright owners. A copy can be downloaded for personal non-commercial research or study, without prior permission or charge. This item cannot be reproduced or quoted extensively from without first obtaining permission in writing from the copyright holder(s). The content must not be changed in any way or sold commercially in any format or medium without the formal permission of the copyright holders.

This document is the author's post-print version, incorporating any revisions agreed during the peer-review process. Some differences between the published version and this version may remain and you are advised to consult the published version if you wish to cite from it.

Energy evaluation of rammed earth walls using long term in-situ measurements

Lucile Soudani^{1,2}, Monika Woloszyn², Antonin Fabbri^{1,*}, Jean-Claude Morel³, Anne-Cécile Grillet²

¹LGCB-LTDS, UMR 5513 CNRS, ENTPE, Université de Lyon, 69100 Vaulx-en-Velin, France ;

²LOCIE, CNRS-UMR 5271, Université Savoie Mont Blanc, Campus Scientifique, Savoie Technolac, 73376 Le Bourget-du-Lac Cedex, France

³School of Energy, Construction and Environment, Faculty of Engineering, Environment & Computing, Coventry University, UK

ABSTRACT: Available throughout the world and used in construction for thousand years, earthen materials are known to improve indoor air quality while keeping the internal temperature relatively stable. In Rhône-Alpes, France, the rammed earth technic is the most spread and consists in compacting layers of earth, one by one, within a framework. Current thermal standards, which are mainly based on thermal resistance of the material, urge to insulate walls. However, due to its interaction with its environment, and its couplings between heat and moisture transfers, the observed thermal behavior of uninsulated rammed earth is commonly significantly above the expectations. The objective of the paper is to highlight the living comfort provided by non-insulated rammed earth walls, for different orientations, from in-situ measurements performed over more than two years. Winter, without or with low energy consumption for heating, and summer, with no cooling device, are studied. The study points out the important role of solar irradiance on the thermal balance of the house, and thus the importance of a good architecture.

1. Introduction

Rammed earth, and more generally earthen materials, is often promoted as a sustainable building material, based on their low embodied energy[1]. As a local material, it can be produced and used immediately on the construction site or nearby and does not require industrial processing. It is not a renewable but a reusable material; it requires no treatment to be reused and therefore has a very low impact in terms of energy consumption. However, they also have a low thermal resistance (R-value), which makes them likely to provide poor thermal performance, as underlined in [2][3]. Indeed, high thermal resistance prevents heat flow from indoor to outdoor climates so that less heating energy is needed to maintain constant indoor temperature, even for high outdoor temperature variations over days and seasons. During the summer, the aim is to prevent outdoor heat from entering as well as to expulse indoor heat to refresh the house during the night. On the other hand, to minimize energy consumption in winter, or more generally when the weather is cold, it is important not only to keep indoor heat but also to capture the maximum amount of outdoor heat during the day so that it can be used during the night when temperature drops. The passive use of solar energy for the heating of buildings is therefore becoming increasingly important and has been the object of many studies since the work of Trombe [4][5]. Solar radiation is a time-dependent energy source which requires an energy storage being able to collect and store heat during the day and release to indoor air when the temperature falls at night, and as a consequence, decreasing indoor temperature swings and improving the thermal comfort level[6]. The thermal energy may be stored in the form of sensible heat in a massive material, to be introduced between direct solar radiation and the living place[7]. Another type of thermal storage system is based on the concept of latent heat storage through phase change

materials (PCM) that are able to store more heat and whose melting temperature ranges from 20°C to 32°C[8]. Indeed, they use chemical bonds to store and release heat when the material changes from solid to liquid and the other way round [8].

In this context, earthen materials, and rammed earth particularly, appear to be able to store both sensible heat as a massive material and latent heat due to liquid to vapor phase changes occurring with the pores. Indeed, several works (e.g. [9]) support that the high thermal mass of the material avoids low temperatures in winter and hot temperatures in summer [10][11]. When exposed to a heat source (internally with heater or externally with solar radiation), the wall absorbs and stores the heat to release it when the surrounding temperature drops[9]. This effect may be enhanced by the so-called hygrothermal couplings between heat and mass transfers which occur within the earthen walls[12].

The following study will use experimental data from a monitored house composed by non-insulated rammed-earth walls to investigate its energy performance over the seasons. In particular, the importance of the solar exposure of the rammed earth walls is questioned for both winter and summer thermal performances. In order to explain these performances, the thermal behavior of the wall, at material scale, is investigated. The aim is to identify parameters needed to evaluate accurately the thermal performance of the material.

2. Monitored house

2.1 Main characteristics

The house studied in this paper is located in Saint-Antoine-l'Abbaye, in Isère, South-Eastern France. It has a living area of 150m², over two floors and cold attics. Its envelope is composed of four non insulated load bearing walls in rammed earth (exposed to the South, East and West) 50cm thick and 3m high and a timber-frame wall filled with straw (mainly North orientation and upper parts of the construction), as it can be seen in Figure 1, Figure 2 and Figure 3. The earth used for the wall construction was taken about 10km away from the site. The slab is made out of a mix of cement, lime, straw, sawdust and cellulose wadding, and covered with fired earth tiles.

Openings count windows and doors described below (according to [13]) :

- Double glazing Argon for South, East and West facades ($U=1.70 \text{ W.m}^{-2}.\text{K}^{-1}$)
- Triple glazing Argon for North façade ($U=1.09 \text{ W.m}^{-2}.\text{K}^{-1}$)
- Double glazing for wooden French window ($U=2.95 \text{ W.m}^{-2}.\text{K}^{-1}$)
- Wooden door ($U=5.00 \text{ W.m}^{-2}.\text{K}^{-1}$)

The house is occupied by five persons (two adults and their three children from 10 to 18 years old). The heating system is a wooden stove operated by the occupants and located in the living room. Yearly energy consumption is evaluated at two cubic meters of wood with the stove turned on two hours a day in winter, early spring and late autumn, which corresponds approximately to 3000kWh according to [14], i.e. $20 \text{ kWh.m}^{-2}.\text{year}^{-1}$ (the surface being the leaving area). Given the size of the house, such consumption is quite low.

During the summer, no cooling system is installed, only natural ventilation is used. Regarding the close environment, a mound of earth is located near the western rammed earth wall.

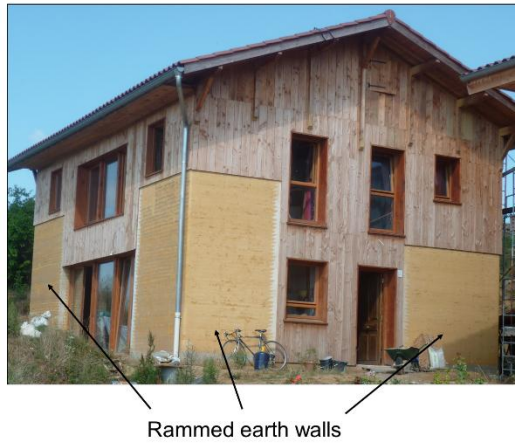


Figure 1 : House in Saint-Antoine-l'Abbaye (2014)

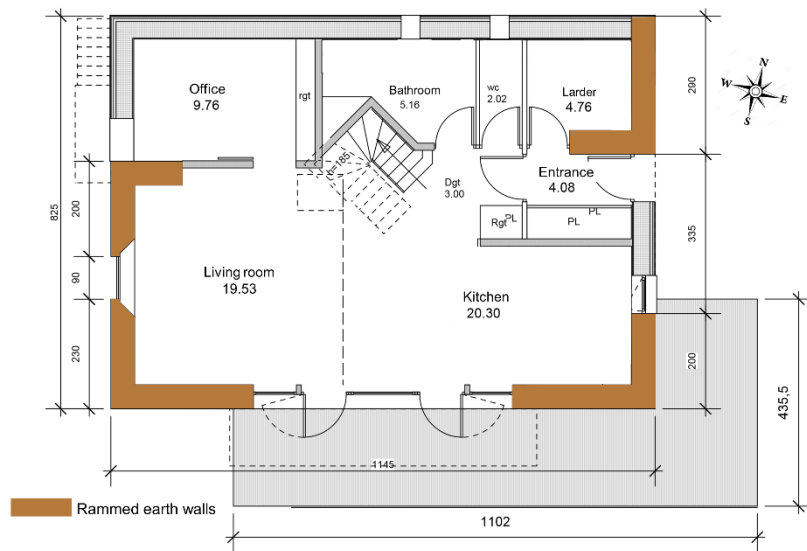


Figure 2: Home plan for the ground floor, with the four rammed earth walls

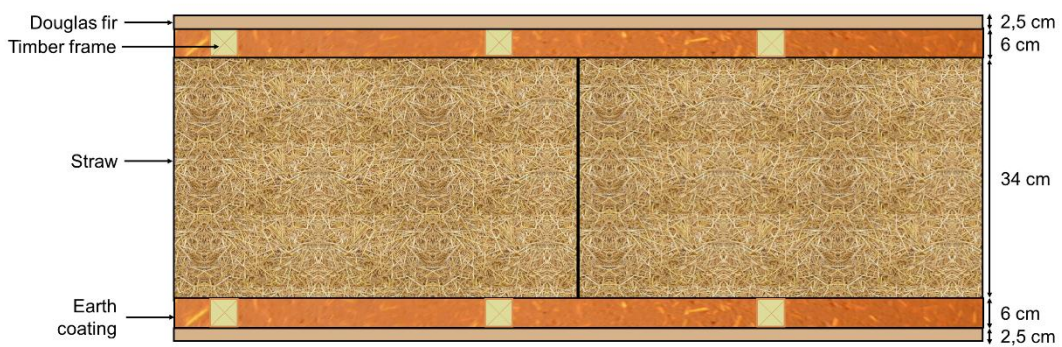


Figure 3 : Composition of non-rammed earth walls and thicknesses

2.2 Instrumentation

The house has been monitored from construction in summer 2011 until now.

12 sensors were placed inside the South/West wall during the construction, at 6 different positions (in the middle and at 10cm from both surfaces), as illustrated in Figure 4 ; their names are gathered in Table 1. At each spot, two sensors were placed: a temperature/relative humidity sensor (CS215, Campbell Scientific, Inc., Logan, UT) and a TDR sensor (CS616, Campbell Scientific, Inc., Logan, UT) to evaluate the water content. The sensors were placed at about 2m from the ground. The measure reading is set to every 15min and the mean value over an hour is saved. An additional temperature/relative humidity sensor (CS215) was placed at the internal surface, in the corner of the South/West wall.

7 sensors for temperature and relative humidity (EL-USB-2, Lascar electronics, Salisbury, UK) were placed inside the house at different locations: in the living room (near the south-west rammed earth wall), in the kitchen (near the south-east rammed earth house), in the WC of the ground floor, and one in each of four bedrooms upstairs. The mean value is saved every hour.

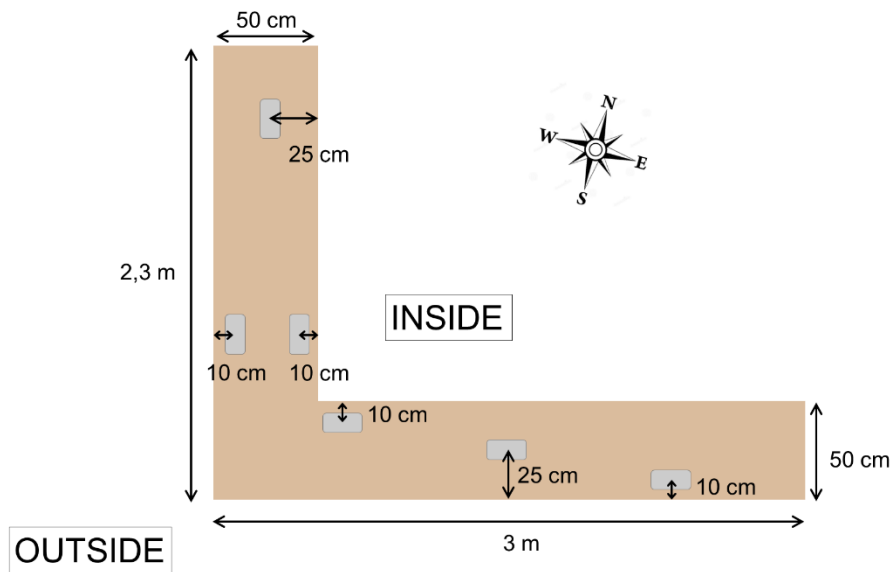


Figure 4: Sensors location in the studied wall

Table 1 : Corresponding names of the sensors

| Name | Location |
|---------------|--|
| $Wext_{wall}$ | in the western wall, at 10 cm from the external surface |
| $Wmid_{wal}$ | In the western wall, in the middle of the wall |
| $Wint_{wall}$ | in the western wall, at 10 cm from the internal surface |
| $Sext_{wall}$ | in the southern wall, at 10 cm from the external surface |
| $Smid_{wall}$ | In the southern wall, in the middle of the wall |
| $Sint_{wall}$ | in the southern wall, at 10 cm from the internal surface |
| Ins | Inside the house, near the wall |
| Out | Outside the house, near the wall |

The weather station installed near the house only records outdoor temperature and relative humidity. The complementary weather data (solar irradiance) was taken from the most complete station in the region located in Vaulx-en-Velin, France [15]. It provides, every minutes and since 1992, a large amount of measurements related to the temperature, relative humidity, sun (light and energy) and wind. The distance of the station to the house location (about 110 km) should be noticed. Therefore, the Vaulx-en-Velin weather station measurements were compared with those from a non-professional

station located in Saint-Marcellin (8 km from the house) and didn't show much difference on the studied periods.

The present study covers the two-year period from March 2013 to June 2015 when the house was occupied.

3. Energy Performance

3.1 General observations

3.1.1 Estimation of heat fluxes using measured data

Energy performance can be quite difficult to quantify as it depends not only on building's intrinsic parameters but also on the occupants and their habits. However, a first sight can be given by the study of heating demand, calculated from the outgoing flux (illustrated as "heat loss" in Figure 5).

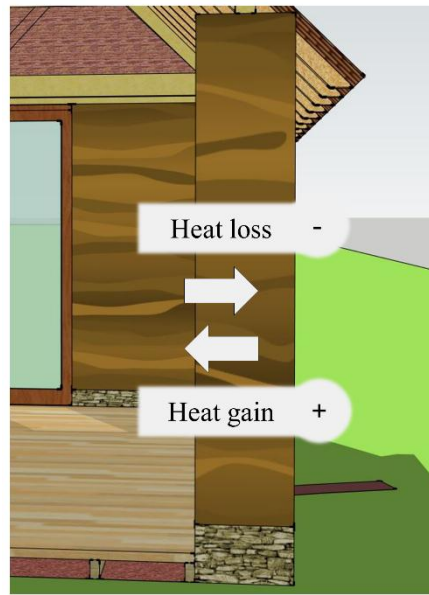


Figure 5 : Sign convention for heat gain and loss in this study

The heat flux ϕ [$\text{W}\cdot\text{m}^{-2}$] through the wall can be calculated using the well-known Fourier's law:

$$\phi = -\lambda \text{grad}(T) \quad (1)$$

In steady conditions, the heat flow is constant throughout the wall. In unsteady, i.e. real conditions, it varies because of the heat storage within the materials. Consequently, at a given time heat flow value can be different in the middle of the wall as well as at the external and internal surfaces. In the present work, we are interested in the value of heat flux exchanged between indoor air and the wall as it impacts directly heating demand. This heat flux is estimated using temperatures measured in the air (one of the EL-USB sensor placed near the wall) and in the wall at 10 cm from the indoor surface:

$$\phi_{gain} = \left(\frac{e}{\lambda} + \frac{1}{h_i} \right)^{-1} \cdot (T_{x_{int_{wall}}} - T_{ins}) \quad (2)$$

with

T_{ins} [°C]: temperature inside the house

$T_{Xint_{wall}}$ [°C]: temperature inside the wall, (here at 10 cm from the internal surface)

X : S for the southern wall and W for the western wall

e [m]: thickness of the layer between the sensor and the surface, i.e. 10 cm

λ [$\text{W}\cdot\text{m}^{-1}\cdot\text{K}^{-1}$]: thermal conductivity of the layer between the sensor and the surface, (here taken equal to $1 \text{ W}\cdot\text{m}^{-1}\cdot\text{K}^{-1}$ according to [12])

h_i [$\text{W}\cdot\text{m}^{-2}\cdot\text{K}^{-1}$]: surface heat transfer coefficient for indoor surface, taken equal to 8 according to [16]

Negative value of heat flux (when indoor air temperature is higher than wall temperature) means that the heat exchanged between the air and the wall is a loss for the room.

3.1.2 Boundary conditions

The heat fluxes through the wall depend mainly on indoor and outdoor temperatures as well as on solar irradiance.

In Figure 6 are reported interior (next to the surface) and exterior temperatures for the entire period from April 2013 to June 2015. These temperatures are, for each month, the mean value of measurements collected every hour. Is also reported the direct horizontal irradiance of the sun. For each month, it corresponds to the mean value of data collected every minute.

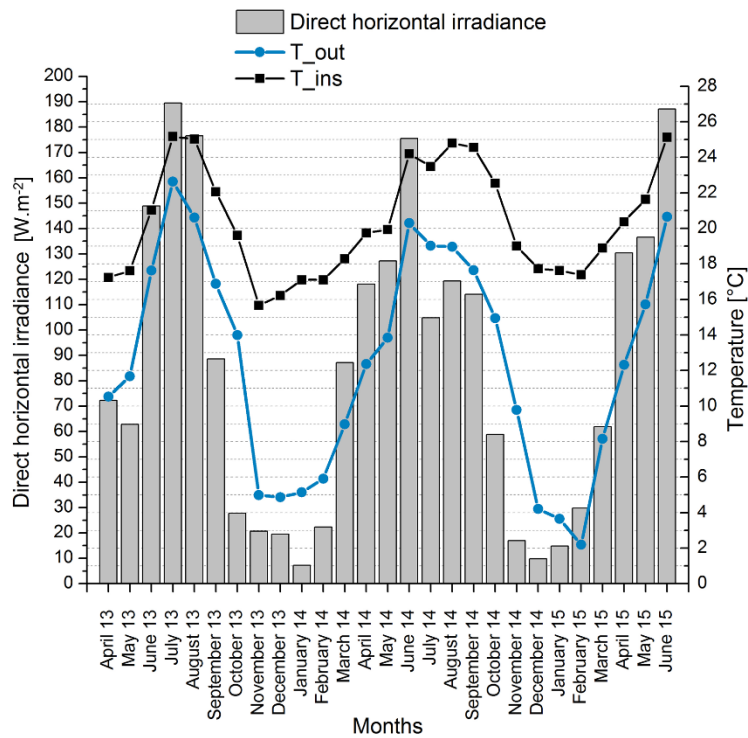


Figure 6 : Outside and inside temperatures and direct horizontal irradiance of the studied period

As expected, it can be noticed that the maximal solar radiation reaches the house in summer and the minimal in winter. However, even for the same season, solar radiation can be different (e.g. July in 2013 and 2014) and this, even if the mean temperature is the same (e.g. October 2013 and May 2014). Solar radiation thus provides an additional information to temperatures. These observations lead to consider, for the different season, periods with “sunny weather” (understood as high direct horizontal irradiance) and “cloudy weather” (understood as low direct horizontal irradiance).

Information provided in Figure 6 gives an interesting overview, however it is not sufficient to study several specific phenomena such as daily variations. For example, as mean values are considered, the inside temperature of summer months is always higher than the outside temperature, the latter not going above 25°C, as well as the winter outside temperature not going below 2°C. To carry out a deeper analysis, the following parts focus on the winter and summer thermal balances, dealing more in details with data just introduced.

To be clearer on the periods considered, in the following analyses, seasons dividing a year in the northern hemisphere as recalled in Table 2.

Table 2 : Seasons in the northern hemisphere

| | |
|---------------|---|
| Spring | March 20 th to June 20 th |
| Summer | June 21 st to September 22 nd |
| Autumn | September 23 rd to December 20 th |
| Winter | December 21 st to March 19 th |

3.2 Thermal balance in winter

First of all, the study of the whole season provides the main tendency. In Figure 7, the thermal balances of both western and southern walls are illustrated, for two winters 13/14 and 14/15. The “heat gain”, respectively “heat loss”, corresponds to the integral in the season of the mean hourly value of negative, respectively positive, flux. The integral is then multiplied by the number of hours in a year, thus enabling a better comparison of the involvement of each season in the annual thermal balance, despite the different number of days considered for each period. The flux can thus be expressed in kWh.m⁻².year⁻¹ (the surface being the vertical surface of the walls). This enables to avoid differences due to.

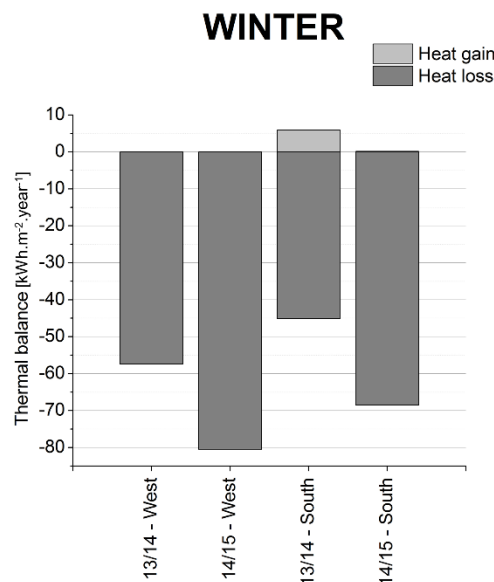


Figure 7 : Thermal balance of West and South walls in winters 2013/14 and 2014/15

The first observation is the majority of heat losses in both orientations and years. Indeed, the temperature is higher inside the house than outside, partly because of the heating system, thus driving out the heat through the wall. But the losses are lower for the southern wall than for the western: the solar radiations heat the wall, which leads to lower the gap between wall surface and inside temperatures, consequently lowering the heat flux. As the southern wall is exposed to the solar radiation earlier in the morning and longer in the daytime, this observation remains intuitive. A

difference is also noticeable between the two winters: the losses are globally more important in 14/15 than in 13/14. This can be explained by the mean weather of each winter, the first being milder than the second. Indeed, although the internal mean temperature is quite similar (17.5°C for winter 13/14 and 17.9°C for winter 14/15), the outside temperature is lower for winter 14/15 (4.7°C) than for winter 13/14 (6.7°C). What's more, looking at Figure 6, the mean monthly irradiance value of winter 13/14 (/per month) is equal to 38.9 W.m⁻² whereas it is 35.5 W.m⁻² for winter 14/15.

At last, the presence of heat gains through the southern wall for winter 13/14 can be noticed, whereas they are almost equal to zero in winter 14/15. The heat gains reach around 13% of the amount of heat losses over the winter 13/14 for the southern wall. It means, that despite lower outside temperature, heat can go from the wall to the inside of the house.

To carry out a deeper investigation, let us focus on three days, among others, when the reversed heat flux occurred, e.g. from March the 9th to March the 12th of 2014. In Figure 8a are represented the hourly total heat flux (positive being heat gain and negative being heat loss) in the southern wall, as well as the direct horizontal irradiance over the same period of time.

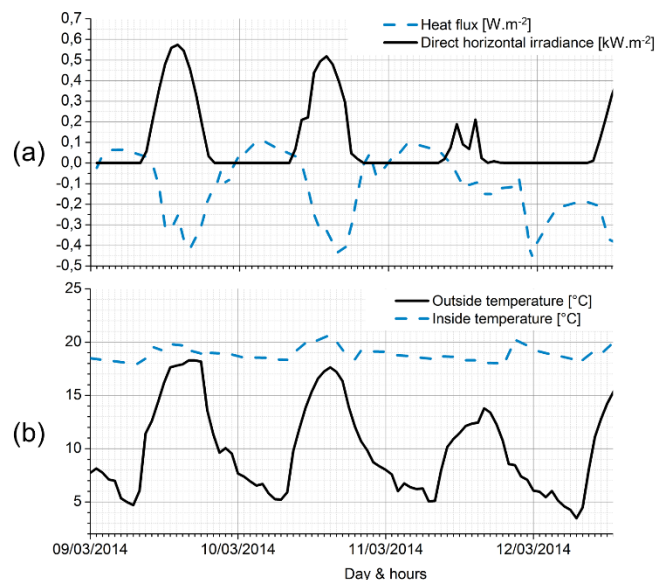


Figure 8 : March 2014 (a) Heat flux in the southern wall against solar irradiance; (b) Inside and outside air temperatures

It can be noticed that the peak of the maximal flux (i.e. the maximal heat gain) always occurs around 4 a.m., whereas the maximum solar irradiance occurs around noon. As soon as the sun goes down (i.e. when the solar irradiance is equal to 0), the heat flux becomes positive. More precisely, the heat gain seems to be proportional to the intensity of the solar irradiance of the daytime before (e.g. on the 9th and 10th, the irradiance is high, so is the heat gain, whereas on the 11th, the irradiance is low and there is no heat gain the night after). This means that the drop of temperature due to the sunset leads to a positive flux within the house: the heat is stored during the day and released during the night.

In Figure 8b, outside and inside temperatures over the same period are represented. It is easily remarkable how the outside temperature is related to the direct horizontal irradiance. On the other hand, the inside temperature remains stable, with the exception of slight increasing which might correspond to owners coming back home and starting the heater and is not related to the solar irradiance peak.

These analysis reveal the energy performance of the house during the cold season which generated comfortable inside temperatures, low heating consumption (most probably below the French Thermal

regulations regarding primary energy), a good thermal mass allowing interesting phase shifts of solar gains and an overall good insulation of the house despite the non-insulated rammed-earth walls.

3.3 Thermal balance in Summer

The other aspect to be kept in mind regarding energy performance of building envelope is the summer comfort, understood here as moderated indoor temperatures when outside temperatures are high.

First of all, an overview of heat fluxes in summer is presented in Figure 9.

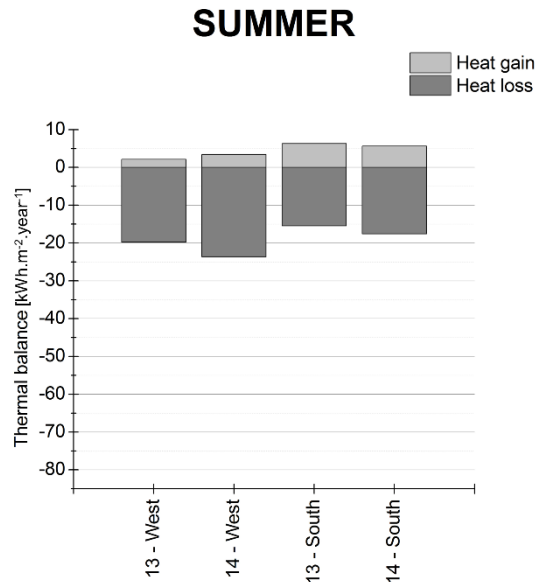


Figure 9 : Thermal balance of West and South walls in summer 2013 and 2014

As the same scale is kept for both Figure 7 and Figure 9, it can easily be noticed that the heat losses are far lower in summer than in winter. Losses are lower and gains higher, for the southern wall than the western wall, for the same reasons as previously detailed. A slight difference in both losses and gains between the two summers can be explained by a more sunny summer 2013. Indeed, looking back at Figure 6, the mean solar irradiance is 152 W.m⁻² in 2013 against 113 W.m⁻² in 2014.

The heat gains are notably low, there is thus no need for any cooling system. More precisely, the heat losses are to be considered as saved energy to cool the room. In order to study more in detail heat fluxes at daily scale, two periods were selected during summer 2013, one qualified as “sunny weather” and the other as “cloudy weather”. They are reported in Table 3.

Table 3 : Selected weeks in summer 2013

| | Periods | Mean daily direct solar irradiance [kWh.m ⁻²] |
|-----------------------|--|---|
| Sunny weather | July 20 th to 27 th 2013 | 5.4 |
| Cloudy weather | June 24 th to 30 th 2013 | 2.8 |

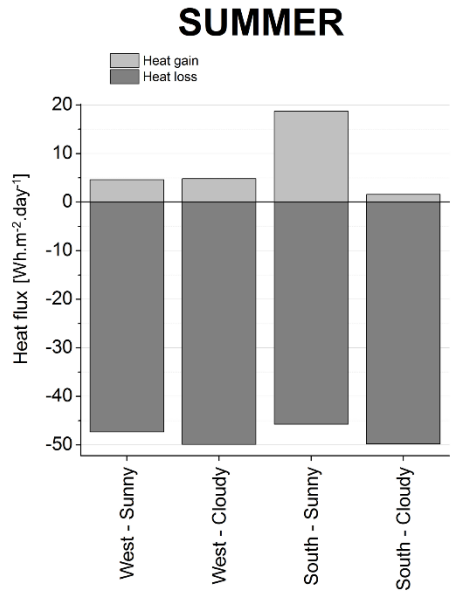


Figure 10 : Daily thermal balance for sunny and cloudy weathers of West and South walls in summer 2013; Mean values are calculated over the corresponding periods

The Figure 10 focuses on the thermal balance of western and southern walls during these two periods. For both orientations, the losses are higher than the heat gains, consequently due to higher indoor than outdoor temperatures. On the other hand, the western wall seems to be less impacted by the decrease of solar irradiance. Indeed, the heat gains are almost the same for both cloudy and sunny weathers. This can be due to the presence of a mound of earth near the western part of the house, as thus preventing it from receiving a part of direct solar irradiance. This raises the importance of the rammed earth walls location to ensure their optimal behavior.

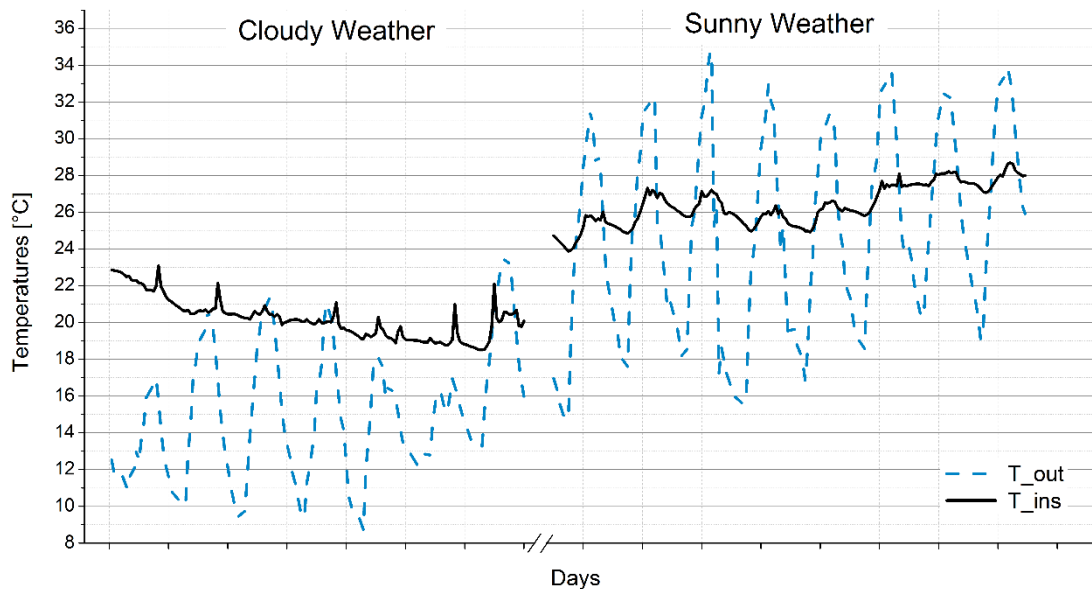


Figure 11 : Inside and outside temperatures for the two weeks referenced as "cloudy" and "sunny" weather during summer 2013

The Figure 11 provides the inside and outside temperatures for the two periods mentioned above. First of all, for both periods, the inside remains at a comfortable level, regarding the outside temperature. Indeed, whereas the outside temperature reaches 35°C, the inside temperature doesn't increase above 28°C. During the "cloudy weather" week, the inside temperature decreases slightly from 23°C to 19°C

in seven days whereas the outside temperature falls beyond 10°C. This highlights the very good thermal mass of rammed earth and the rather good insulation of the house.

The results clearly show excellent stability of indoor temperatures: daily variations are lower than 2°C. Such stable indoor climate in an occupied dwelling is clearly an advantage of the house and demonstrates its high thermal mass.

4. Thermal behavior of the wall

Temperature profiles in the wall are functions of the inside and outside temperature, as well as of the thermophysical properties of the materials. The heat wave on the outer surface of the wall travels through the wall and its deformation depends on the material properties. It reaches the inner surface, with a smaller amplitude and after a certain time. The taken time is named “time lag” (see eq(3)) and the ratio of the two amplitudes is known as “decrement factor” (see eq(4)). Associated with the thickness, time lags and decrement factors are very useful characteristics to quantify the heat storage capacities of a wall.

The thermal mass of a material is related to its abilities to store and release the heat with its surroundings, and thus depends on how fast the heat is absorbed and distributed. Parameters usually used are the diffusivity and, at some point, the effusivity. They enable to quantify heat exchanges for different materials.

In the following paragraphs, the results of experimental measurements are given, then a more detailed analysis is conducted on time lag, decrement factor as well as on thermal diffusivity and effusivity.

4.1 Time lag and decrement factor

As already mentioned above, measurements through seasons reveal different phenomena occurring within the rammed earth wall: the outside temperature and its variations are not only lowered when passing through the wall, but also delayed, thus inducing a time lag in temperature transmission. Those phenomena depend on the material properties, and can be related to its thermal mass.

In order to provide an overview of the thermal behavior of rammed earth walls, the following study focuses on the whole year 2014, divided in four seasons.

Figure 12 is composed by 4 graphs, each one representing temperature variations for a typical week in each season. On each graph, there are 4 temperature distributions corresponding to the internal and external temperatures in the wall, and the outside and inside temperatures of the air near the wall. Only the southern wall is represented here, as the tendencies are similar for the western wall.

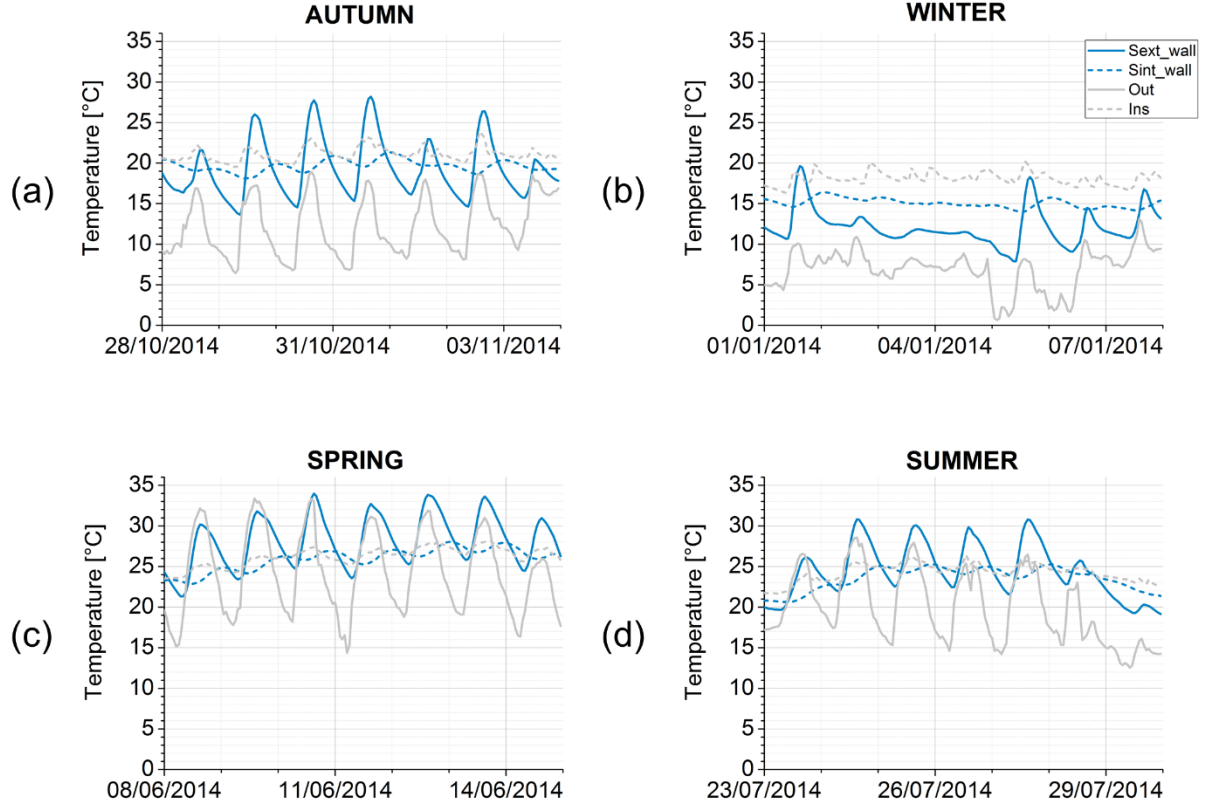


Figure 12: Wall and air temperatures in and near the southern wall along the year 2014

For each season and each orientation, the two phenomena of time lag and temperature buffering can be observed. The following analysis will focus on their quantification depending on the orientation of the wall and the season.

The decrement factor (DF) is defined as:

$$DF = \frac{T_{ins}^{max} - T_{ins}^{min}}{T_{out}^{max} - T_{out}^{min}} \quad (3)$$

while the time lag (TL) is:

$$TL = t_{T_{ins}^{max}} - t_{T_{out}^{max}} \text{ with } t_{T_{ins}^{max}} > t_{T_{out}^{max}} \quad (4)$$

where $t_{T_{out}^{max}}$ is the time of the external temperature peak and $t_{T_{ins}^{max}}$ is the time of the following internal temperature peak. We assume here that TL cannot be equal to zero. In consequence, if the peaks of internal and external temperature occur at the same time, TL is taken equal to the period of the temperatures oscillations.

In order to facilitate the comparison, the numerical values of the decrement factor from the external to the internal value of temperature in the wall, as well as the time lag between the two peaks are reported in Figure 13. The graphs (a) and (b) deal with the time lag and decrement factor of western and southern walls.

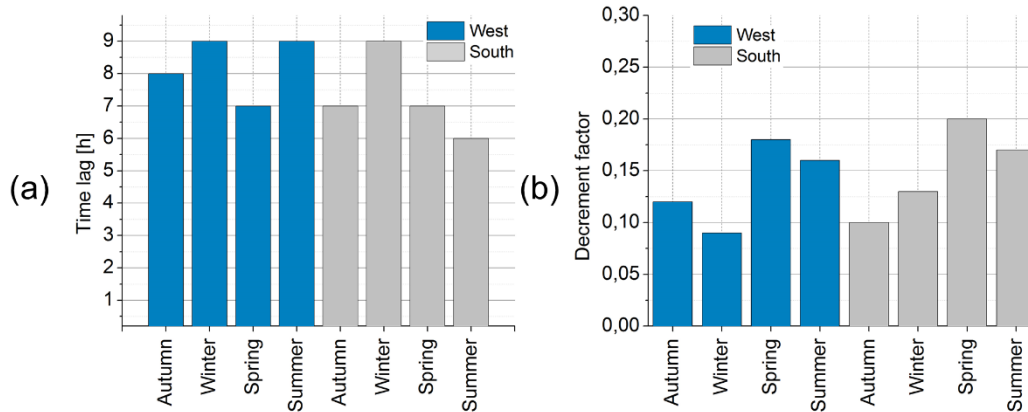


Figure 13: (a) Time lag; (b) Decrement factor

4.1.1 A non-season nor orientation dependent time lag

As it can be noticed in Figure 13(a), for all seasons and orientations, the time lag between external and internal temperatures is important: it varies from 6 to 9 hours, with a mean value of about 8 hours. However, care should be taken when considering the precision of the given values as the data is collected every hour, being the mean value of 6 measurements.

For all seasons, the daily temperature variations can be observed in Figure 12. A time lag can be noticed between temperatures near the exterior and interior surfaces: the inside temperature reaches its maximum on average 8 hours after the outside temperature. Given the precision of the values, this time lag doesn't seem to depend on the seasons nor the orientation of the wall: it may be related to the material properties. This observation follows theoretical results, as developed in the literature, for example in [17] or [18].

However, another time lag can be measured between the temperature variation of the western wall and southern wall (around 3 hours on average), when comparing the western and southern data (not clearly visible in Figure 13). This difference might be due to the variation of the sun position (taking the Earth as a reference) during the day: the southern wall is exposed earlier in the morning all day long whereas the western wall is in the shade in the early morning; even more considering the mound of earth located near the western wall and masking the sun earlier in the afternoon.

4.1.2 Temperature buffering and decrement factor

In Figure 12, for all seasons, a decrement factor is observable in terms of temperature: the effect of the external temperature is lowered and buffered by the wall. During the selected periods, the maximum temperature difference between the internal and external position of the wall reaches 7°C. In the same graph, the comparison of extremum temperatures is interesting. Indeed, whereas the external temperature reaches 35°C, the maximal internal temperature is 26°C. On the contrary, when the external temperature of winter reaches 6°C, the minimal internal temperature is 14°C.

In Figure 13b, the decrement factor varies from 0.09 to 0.20, which can be considered as low in comparison with other wall's compositions studied experimentally in [19] (from 0.24 to 0.41). What's more, the decrement factor seems to depend on the amplitude variation of the external temperature, as the internal temperature tends to reach the more stable variation. Indeed, even if high or low temperatures are measured in the external position, the temperature measured in the internal position is stable (low variation during the day), as it is drawn in Figure 12. However, data from cool season

should be analyzed with care as the heating device, even low as it was, have an impact on the decrement factor.

In the literature, many authors studied the variation of decrement factor depending on the material parameters and wall thickness [20], [21]. It appears that the amplitude of the heat wave on the outer surface of the wall influences the decrement factor.

4.2 Thermal mass of the wall

Previous observations highlight the strong potential of rammed earth wall to buffer temperature variations and to establish a time lag in temperature transmission into the house. According to the theory, the experimental data as well as the literature, these phenomena seem to depend on the material properties themselves.

4.2.1 Effusivity and diffusivity

When a material is at equilibrium with its environment, its temperature is constant and heat exchanges are equilibrated. Thermal mass is the ability of the material to keep its initial temperature when subjected to a perturbation. If the perturbation tends to bring the material to a new equilibrium temperature, thermal mass represents how long it will take to reach this new equilibrium. The higher the thermal mass is, the slower the transition will occur. Correspondingly, temperature buffering and time lag increase with the thermal mass.

Two parameters are often used to quantify thermal mass of a construction material: diffusivity D [$\text{m}^2 \cdot \text{s}^{-1}$] and effusivity E [$\text{J} \cdot \text{kg}^{-1} \cdot \text{m}^{-2} \cdot \text{s}^{-1/2}$].

The thermal diffusivity is defined as the ratio between the thermal conductivity and the product of the density with the thermal capacity. It thus reflects the ability of the material to transmit temperature variations; it characterizes the speed of calories displacement. The lower the diffusivity is, the higher are the buffering effects of the material.

$$D = \frac{\lambda}{\rho C_p} \quad (5)$$

With

λ [$\text{W} \cdot \text{m}^{-1} \cdot \text{K}^{-1}$]: thermal conductivity of the layer between the sensor and the surface

ρ [$\text{kg} \cdot \text{m}^{-3}$]: dry density

C_p [$\text{J} \cdot \text{kg}^{-1} \cdot \text{K}^{-1}$]: thermal capacity at constant pressure

The thermal effusivity is defined as the square root of the product of the thermal conductivity, density and thermal capacity. It is a measure of the ability of the material to exchange energy with its surroundings and to absorb calories. The higher the effusivity is, the more quickly the material absorbs heat without temperature rise at its surface.

$$E = \sqrt{\lambda \rho C_p} \quad (6)$$

It is interesting to compare these coefficients for different building materials and to study the place of earthen materials. Let us note here that the parameters can vary for each material and that the values used, being standard ones, endeavor to be as realistic as possible. As their sensitivity to water is well known, two earthen materials will be considered in the following: dry and wet earth, with a mass water content of 10%.

Table 4 : Building material parameters used to calculate diffusivity and effusivity according to [22] and [23]

| Materials | Thermal conductivity [W.m ⁻¹ .K ⁻¹] | Density [kg.m ⁻³] | Specific heat [J.kg ⁻¹ .K ⁻¹] | Diffusivity [m ² .s ⁻¹] | Effusivity [J.kg ⁻¹ .m ⁻² .s ^{-1/2}] |
|-----------------|--|-------------------------------|--|--|--|
| Wood fiber | 0.04 | 160 | 2100 | 1.2e-7 | 116 |
| Wood (fir) | 0.15 | 500 | 1600 | 1.9e-7 | 346 |
| Gypsum | 0.25 | 825 | 1000 | 3.0e-7 | 454 |
| Dry earth | 0.6 | 1730 | 648 | 5.4e-7 | 820 |
| Solid brick | 0.74 | 1800 | 1000 | 4.1e-7 | 1154 |
| Wet earth (10%) | 1.1 | 1730 | 648 | 6.4e-7 | 1158 |
| Stone | 1.7 | 2000 | 1000 | 8.5e-7 | 1844 |
| Solid concrete | 1.8 | 2300 | 1000 | 7.8e-7 | 2035 |

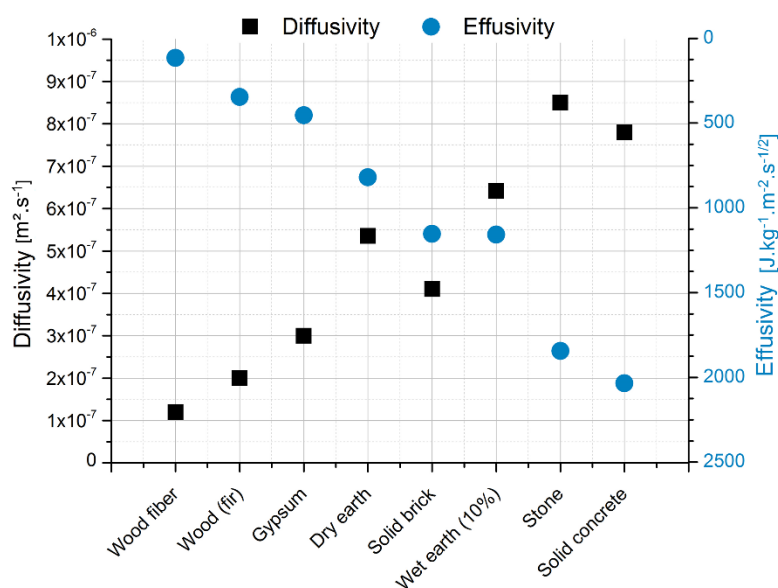


Figure 14 : Diffusivity and effusivity for different building materials

One way of improving thermal performance of a building material, is to find a good compromise between a low diffusivity and a high effusivity.

Looking more in details at Figure 14 and Table 4, it can be noticed that materials such as wood or gypsum have a very low diffusivity but a high effusivity: they will be able to buffer temperature variations but not to store heat efficiently. On the contrary, materials such as solid concrete or stone, have a high effusivity but a low diffusivity: they will be able to absorb heat without temperature rise in surface, but will transmit heat quickly and the outside temperature variations won't be lowered by the material. It is necessary to highlight the fact that the parameters used to compare these building materials are standard one, and can vary from the values given in Table 4. Finally, earthen materials, dry, wet or fired (solid brick), seem to offer both a low diffusivity and a high effusivity (located in the central part of the graph).

4.2.2 Link with time lag and temperature buffering

A material which induces high time lags and low decrement factors provides almost constant inside temperatures which results in a good comfort level. This has been stated by many authors [17], [21], [24]. These characteristics have to be imputed to material parameters such as thermal conductivity and thermal capacity, which are thus indirectly related to the diffusivity and effusivity previously

presented. Several studies investigate the relationship between these parameters and the induced time lags and decrement factors.

In [20], a numerical study over twenty-six building materials explores the influence of the thermal diffusivity, the heat capacity and the thickness of the walls. It reveals that “materials with high thermal diffusivity give considerable lower time lags than materials with small diffusivity”, as well as “materials with high heat capacity and high thermal conductivity [...] give considerable lower time lags”. Regarding the decrement factor, it seems to get lowered by greater thicknesses, greater heat capacities and low diffusivity.

In [25], time lags and decrement factors are used to evaluate the thermal performance of a wall. Here again, increasing the thermal conductivity leads to a decrease of time lag and the increase of the decrement factor. The increase of thermal capacity leads to the increase in time lag and decrease in decrement factor. The increase of thickness leads to the increase in time lag and the decrease in decrement factor.

These observations are in accordance with the previously made study regarding effusivity. A good thermal performance requires a high effusivity which grows with the increasing of thermal capacity and thermal conductivity.

4.2.3 Heat storage capacity of the rammed earth walls

This section focuses on the temperature profile variations through the day. It is observed for two seasons: winter and spring. The data from the three sensors in the wall as well as the outside and inside temperatures are represented in Figure 15, at different times during a whole day.

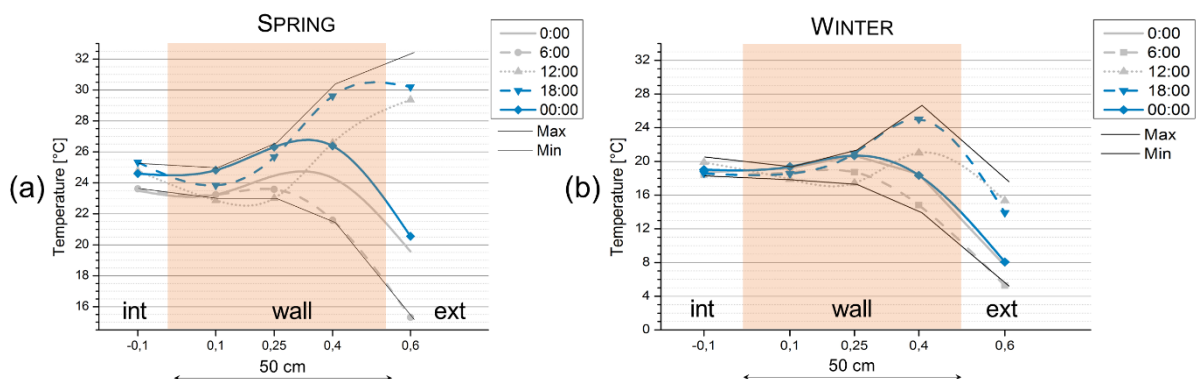


Figure 15 : (a) Wall section of the southern wall for the winter (January 1st 2014); (b) Wall section of the southern wall for the spring (June 8th 2014)

In Figure 15a, during the spring, the temperature buffering can easily be noticed with the extremum temperature profiles. The heat propagation from the external surface to the interior of the wall is observable when comparing profiles at 12:00 and 18:00: the outside temperature rise leads to an increase of the temperature in the external part of the wall, with a delay related to the thermal mass.

In Figure 15b, during the winter, the outside temperature is always lower than the inside temperature and the temperature buffering previously mentioned can also easily be observed. However, a part of the wall reaches a higher level of temperature than both maximum inside and outside temperatures. The accumulation of heat is discernable when comparing profiles at 12:00 and 18:00. On the other hand, the comparison of the profiles at 18:00 and the following 00:00 reveals the time lag with which the heat wave is transmitted through the wall.

These two profiles give evidence of the capacity of the rammed earth wall to store a large amount of heat, taking advantage of the surrounding heat sources, including the sun. This feature is linked to the

ratio of diffusivity and effusivity previously mentioned. However, the thermal modeling of the wall could be improved by taking account of the radiation in the boundaries. Moreover, the influence of the coupling between thermal and hygric behaviors should be carefully considered, as suggested by [26].

5. Conclusion

Experimental results from rammed earth walls in a real occupied house were presented and analyzed. The first part of this study focuses on the energy evaluation of the house through the seasons and compares wall orientations. The house provides a good comfort in summer, judging with regards to stability and level of temperatures. Moreover, it offers a good energy performance in winter as the temperature remains comfortable with a very low heating load. Findings confirm good thermal mass of the studied walls and an overall good insulation of the house. The impact of the orientation is also discussed, thus highlighting the importance of architecture for rammed earth houses.

The second part focuses more precisely on the thermal behavior of the walls, revealing important time lags and low decrement factors, which constitute an explanation of the thermal performance illustrated in the first part. These phenomena are related to the thermal properties of the materials, and can be more precisely correlated with common coefficients such as thermal diffusivity and effusivity.

However, the thermal parameters of usual building materials are rather constant, thus making its behavior easier to predict. However, in the case of rammed earth, the thermal parameters are function of the amount of water located in the porous media. A difference is even already remarkable in Figure 14 when dry earth and wet earth lead to different value of diffusivity and effusivity. A study of the influence of the water content on the thermal behavior of the rammed earth walls is to be conducted. The hygrothermal couplings can be an additional element to analyze the thermal behavior, and more generally the energy performance, of the house.

Acknowledgements

We would like to thank Cyrille Lemaitre and his family for their time and help to provide us such data from their house, as well as Nicolas Meunier, the mason who built the house, and Pierre-Antoine Chabriac, Jean-Paul Laurent and Erwan Hamard, who handled the instrumentation ; at last, Pernelle Vodinh and Justine Toulouse for their master work on the same house [13].

The present work has been supported by the French Research National Agency (ANR) through the “Villes et Bâtiments Durables” program (Project Primaterre n°. ANR-12-VBDU-0001).

Bibliography

- [1] J. C. Morel, A. Mesbah, M. Oggero, and P. Walker, “Building houses with local materials : means to drastically reduce the environmental impact of construction,” *Build. Environ.*, vol. 36, pp. 1119–1126, 2001.
- [2] A. Delsante, “A comparison of accurate predictions with measured data from a mud brick house,” in *IBPSA Australasia 2006 Conference*, 2006, pp. 96–103.
- [3] CSIRO, “Mud walls give poor insulation,” 2000.
- [4] F. Trombe, “Maisons solaires,” *Tech. l'ingénieur*, vol. 3, pp. 375–382, 1974.

- [5] Z. Zrikem and E. Bilgen, "Theoretical study of a composite Trombe-Michel wall solar collector system," *Sol. Energy*, vol. 39, no. 5, pp. 409–419, 1987.
- [6] E. Stephan, "Méthode d'aide à la décision multicritère des stratégies de réhabilitation des bâtiments anciens en pierre calcaire - Application au patrimoine en tuffeau," ENTPE, Université de Lyon, 2014.
- [7] Y. Zhang, G. Zhou, K. Lin, Q. Zhang, and H. Di, "Application of latent heat thermal energy storage in buildings : State-of-the-art and outlook," *Build. Environ.*, vol. 42, pp. 2197–2209, 2007.
- [8] V. V. Tyagi and D. Å. Buddhi, "PCM thermal storage in buildings : A state of art," *Renew. Sustain. Energy Rev.*, vol. 11, no. 2007, pp. 1146–1166, 2005.
- [9] P. Taylor and M. B. Luther, "Evaluating rammed earth walls: a case study," *Sol. Energy*, vol. 76, no. 1–3, pp. 79–84, Jan. 2004.
- [10] J. L. Fernandez, M. A. Porta-Gandara, and N. Chargoy, "Rapid on-site evaluation of thermal comfort through heat capacity in buildings," *Energy Bui*, vol. 37, pp. 1205–1211, 2005.
- [11] N. Aste, A. Angelotti, and M. Buzzetti, "The influence of the external walls thermal inertia on the energy performance of well insulated buildings," *Energy Build.*, vol. 41, pp. 1181–1187, 2009.
- [12] L. Soudani, A. Fabbri, J.-C. Morel, M. Woloszyn, P.-A. Chabriac, and A.-C. Grillet, "Assessment of the validity of some common assumptions in hygrothermal modelling of earth based materials Energy and Buildings," *Energy Build.*, 2016.
- [13] P. Vodinh and J. Toulouse, "Etude du comportement thermique d'une maison en pisé," LOCIE, Université de Savoie, 2015.
- [14] ADEME, "Se chauffer au bois," 2015.
- [15] ENTPE, "SATELLIGHT station : IDMP, Vaulx-en-Velin, France." [Online]. Available: <http://idmp.entpe.fr/vaulx/mesfr.htm>.
- [16] H. M. Künzle, "Simultaneous heat and moisture transport in building components one - and two-dimensional calculation using simple parameters - Report on PhD thesis, Fraunhofer Institute of Building Physics," 1995.
- [17] C. Sun, S. Shu, G. Ding, X. Zhang, and X. Hu, "Investigation of time lags and decrement factors for different building outside temperatures," *Energy Build.*, vol. 61, no. 2013, pp. 1–7.
- [18] J. L. Therkeld, *Thermal environmental engineering*. Engelwood Cliffs, Prentice-Hall, 1970.

- [19] K. Ulgen, "Experimental and theoretical investigation of effects of wall's thermophysical properties on time lag and decrement factor," *Energy Build.*, vol. 34, pp. 273–278, 2002.
- [20] H. Asan, "Numerical computation of time lags and decrement factors for different building materials," *Build. Environ.*, vol. 41, pp. 615–620, 2006.
- [21] S. F. Larsen, G. Lesino, and A. History, "Thermal behavior of building walls in summer : Comparison of available analytical methods and experimental results for a case study," *Build. Simul.*, no. 2009, pp. 3–18, 2002.
- [22] PassivAct, "Qualité thermique comparées des matériaux," 2012. [Online]. Available: <http://passivact.com/Infos/InfosConcepts/files/QualiteThermique-ComparaisonsMateriaux.html>.
- [23] P.-A. Chabriac, "Mesure du comportement hygrothermique du pisé," ENTPE, Université de Lyon, France, 2014.
- [24] H. Asan and Y. S. San, "Effects of Wall's thermophysical properties on time lag and decrement factor," *Energy Build.*, vol. 28, pp. 159–166, 1998.
- [25] X. Jin, X. Zhang, Y. Cao, and G. Wang, "Thermal performance evaluation of the wall using heat flux time lag and decrement factor," *Energy Build.*, vol. 47, no. 2012, pp. 369–374.
- [26] M. Labat, M. Woloszyn, G. Garnier, and J.-J. Roux, "Dynamic coupling between vapour and heat transfer in wall assemblies : Analysis of measurements achieved under real climate," *Build. Environ.*, vol. 87, pp. 129–141, 2015.